Theoretical investigation of the scanning tunnelling microscope image of graphite

1990 J. Phys.: Condens. Matter 2 3811

(http://iopscience.iop.org/0953-8984/2/16/011)

J. Phys.: Condens. Matter 2 (1990) 3811–3821. Printed in the UK

Theoretical investigation of the scanning tunnelling microscope image of graphite

D Lawunmi and M C Payne
Cavendish Laboratory, Madingley Road, Cambridge CB3 0HE, UK

Received 19 October 1989, in final form 24 January 1990

Abstract. In this paper, the effects of tunnelling from the p states of the scanning microscope tip are considered. In the case of the graphite surface, it is shown that an appreciable tunnel current flows to the p_x and p_y components of the tip wavefunction and that this tunnel current significantly reduces the amplitude of the corrugations that should be measured on this surface. The results also show that the giant corrugations observed in scanning tunnelling microscope images of graphite cannot be explained by a tunnelling model.

1. Introduction

The surface of graphite has been extensively studied with the scanning tunnelling microscope (STM). A number of these studies have found that the STM image of this surface is characterised by giant corrugations ranging in magnitude from approximately 1 Å to about 10 Å (Binnig *et al* 1985, Elings and Wudl 1987, Colton *et al* 1987). Other studies have reported corrugation amplitudes that are significantly greater than this (Mamin *et al* 1986, Morita *et al* 1987). It is important to know whether these giant corrugations are a genuine tunnelling image of the surface or whether some other phenomenon is responsible for the large magnitude of the measured corrugations. A theoretical analysis of the STM image of graphite (Tersoff 1986) concluded that the giant corrugations could be explained by the electronic structure of the surface. However, this analysis took only the tunnelling to the s state of the STM tip into consideration. The Fermi surface of graphite is a point at the corner of the surface Brillouin zone and the electronic wavefunctions at the Fermi level in graphite are characterised by hexagonal arrays of nodes.

Tunnelling to the s state of the tip is forbidden by symmetry when the centre of the probe is positioned over a node of a surface wavefunction, see figure 1(*a*). The maximum current to the s state is obtained when the tip is above an antinode in the surface wave function as shown in figure 1(*b*). In constant current imaging modes the absence of any tunnel current when the STM tip is positioned above a node of the surface wavefunction will cause the probe to move a large distance towards the surface at this point. Hence Tersoff predicted that there would be giant corrugations in the tunnelling image of the graphite surface (Tersoff 1986). However, tunnelling is permitted to the p states of the tip when the centre of the probe is positioned over a node of the surface wavefunction, see figure 1(*c*). The tunnelling current to the p_x state of the tip wavefunction will attain its maximum value when the tip is positioned above a node in the surface wavefunction,

0953-8984/90/163811 + 11 $03.50

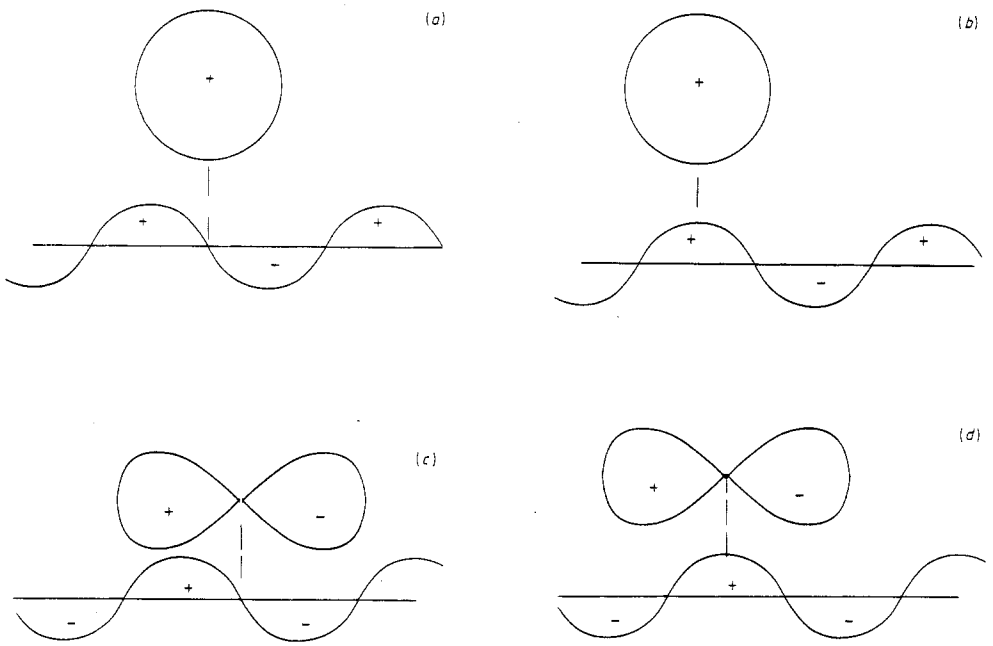

Figure 1. A comparison of the tunnelling current to the tip s and the tip p_x states: a schematic illustration of the wavefunctions of a surface and a scanning tunnelling microscope tip. (*a*) Tunnelling from the surface to the s wavefunction of the tip is forbidden when the tip is positioned over a node of the surface wavefunction. (*b*) The tunnelling current to the tip s state reaches its maximum value when the tip is positioned above an antinode in the surface wavefunction tip at this point. (*c*) In contrast the tunnelling current to the tip p_x state reaches its maximum value when the tip is positioned above a node in the surface wavefunction. (*d*) Tunnelling to the p_x wavefunction of the tip is forbidden when the tip is above an antinode in the surface wavefunction.

the tunnelling current to the p_x state of the STM tip wavefunction will be zero when the tip is positioned above an antinode in the surface wavefunction; see figure 1(*d*).

In constant tunnel current imaging mode the tunnel current to the p states of the tip will prevent the STM probe undergoing a large displacement towards the surface when the tip is over a node in the surface wavefunction. The calculations presented in this paper show that when tunnelling to the p states of the tip is taken into consideration the corrugation amplitude expected in STM images of graphite is extremely small in contrast to the infinite value predicted by Tersoff.

An alternative explanation for the presence of giant corrugations in STM images of graphite has been developed by Pethica (1986). This model is based on contact between the STM tip and the graphite surface. Binnig and Quate (1986), have shown that it is possible to produce an 'STM image' of graphite by making contact between the tip and the surface. Pethica has argued that all that is required to form an STM image in the constant current mode is a fluctuation in the conductivity between the tip and the sample and has shown that STM images of graphite which exhibit giant corrugations can be accounted for by a contact model. It is important to determine whether giant corrugations in an STM image of the graphite surface could be produced purely by tunnelling. If giant corrugations cannot be explained by tunnelling it must be concluded that when STM

images of graphite are characterised by giant corrugations the STM tip has made contact with the surface.

In the following section, Tersoff and Hamann's model for the STM (Tersoff and Hamann 1985) is briefly described. Analytic expressions for the asymptotic forms of the wave are given in section 3. In section 4 these wavefunctions are used to compute the tunnel currents in the STM. In section 5, values are given for the corrugation amplitudes expected to be measured by the STM on a graphite surface.

2. The Tersoff and Hamann model for the STM

A number of models have been proposed for calculating the magnitude of the tunnel current in the STM. However, the most widely used and the simplest to apply is the Spherical tip model of Tersoff and Hamann (1983). They used Bardeen's transfer Hamiltonian formalism (Bardeen 1961) to calculate the tunnelling current between the surface and the tip. The Bardeen matrix elements are given by the following expression:

$$M_{\text{tip,surf}} = [h^2/(8\pi^2 m)] \int \mathrm{d}s \, (\Psi_{\text{surf}} \nabla \Psi^*_{\text{tip}} - \Psi^*_{\text{tip}} \nabla \Psi_{\text{surf}}) \tag{1}$$

where Ψ_{tip} and Ψ_{surf} are wavefunctions of the STM tip and the surface respectively. Tersoff and Hamann applied this formalism in the low bias, low temperature limit to calculate the STM tunnel current. The tunnel current is given by

$$I = (8\pi^2 e^2 V_{\text{bias}}/h) \sum_{\text{tip,surf}} |M_{\text{tip,surf}}|^2 \delta(E_{\text{tip}} - E_{\text{F}}) \, \delta(E_{\text{Surf}} - E_{\text{F}}) \tag{2}$$

where V_{bias} is the voltage applied between the STM probe and the surface, and E_{F} is the Fermi energy.

In the Tersoff–Hamann model, the STM tip is modelled by a spherical square well and only tunnelling to the s state of the tip is included. This model gives the particularly simple result that the contribution to the tunnel current from a particular surface wavefunction, Ψ_{surf}, is proportional to the charge density generated by that wavefunction at the position of the centre of the spherical tip. The total tunnel current is determined by summing up the charge densities generated by all the surface wavefunctions that lie in an energy range eV_{bias}. In the case of the graphite surface at low bias, the surface wavefunctions have nodes at a hexagonal array of points on the surface. Using Tersoff and Hamann's model Tersoff predicted that an STM image of a graphite surface would show giant corrugations because there would be no tunnel current to the STM tip at the points on the surface where the surface wavefunctions have nodes. However, it is obvious that tunnelling can occur to the p_x and the p_y components of the tip wavefunction when the probe is positioned over the nodes of the surface wavefunctions. The tunnel current to these states will reduce the magnitude of the corrugation amplitude from that predicted when only tunnelling to the s state of the tip is included. Tersoff and Hamann (1985) and Lang (1985) have claimed that tunnelling to the p_x and p_y states of the tip that have their nodes directed towards the surface is suppressed because the tunnelling distance is larger than it is for tip wavefunctions that are directed towards the surface. In the following sections, it will be shown that this claim is incorrect.

3. The wavefunctions of the STM tip

In order to calculate the Bardeen matrix elements for tunnelling between the surface and the higher angular momentum components of the tip wavefunction, it is necessary to have analytical expressions for the wavefunctions of the tip. The exact nature of the STM tip is uncertain and therefore a model for the tip must be used. The model conventionally chosen is that of a spherical square well. When the centre of the sphere is positioned at the origin, the wavefunctions for the spherical square well can be written as

$$\Psi_{sw} = C_{l,m} j_l(kr) Y_{l,m}(\theta, \varphi) \qquad r < R \tag{3}$$

$$\Psi_{sw} = C'_{l,m} k_l(\kappa r) Y_{l,m}(\theta, \varphi) \qquad r > R \tag{4}$$

where j_l and k_l are spherical Bessel functions and modified spherical Bessel functions respectively; l is the orbital angular momentum quantum number; m is the azimuthal quantum number; $C_{l,m}$ and $C'_{l,m}$ are normalisation constants and k is equal to $2\pi\sqrt{(2mE)}/h$, where E is the energy of the state, $\kappa = 2\pi(2m\Phi)^{1/2}/h$, where Φ is the work function, and R is the radius of the well.

In the vacuum region the s wavefunction of the spherical square well can be written as

$$\Psi_s = C_s \exp(-\kappa|\boldsymbol{r} - \boldsymbol{r}_0|)\kappa R \exp(\kappa R)/\kappa|\boldsymbol{r} - \boldsymbol{r}_0| \tag{5}$$

where r_0 is the position of the centre of the well and C_s is a normalisation constant. The asymptotic forms of the p wavefunctions of the spherical square well in the vacuum region are given by the following expression:

$$\Psi_{pi} = C_{pi} \exp(-\kappa|\boldsymbol{r} - \boldsymbol{r}_0|)|i - i_0|\kappa R \exp(\kappa R)(1 - 1/\kappa|\boldsymbol{r} - \boldsymbol{r}_0|)/\kappa|\boldsymbol{r} - \boldsymbol{r}_0|^2 \tag{6}$$

where $i = x$, y, or z and C_{pi} is a normalisation constant.

The surface wavefunctions of periodic surfaces are most conveniently expanded in terms of a basis set consisting of plane waves parallel to the surface. In order to simplify the calculation of the Bardeen matrix elements the tip wavefunctions will be expressed in terms of the same basis set. In terms of this basis set the s state of the spherical square well can be written as

$$\Psi_s = C_s \int \mathrm{d}\boldsymbol{q} \exp[-(\kappa^2 + q^2)^{1/2}|z - z_0|] \exp(\mathrm{i}\boldsymbol{q} \cdot (\boldsymbol{x} - \boldsymbol{x}_0))\kappa R$$

$$\times \exp(\kappa R)/[2\pi\kappa^2(1 + q^2/\kappa^2)^{1/2}] \tag{7}$$

where $\boldsymbol{q}$ is a wavevector parallel to the surface, $\boldsymbol{x}$ is a two-dimensional vector parallel to the surface, the z direction is perpendicular to the surface and $(\boldsymbol{x}_0, z_0)$ is the position of the centre of the spherical square well.

The effects of higher angular momentum states on the tunnelling current have also been considered by Chung *et al* (1987) and Chen (1988).

The analysis of Chung *et al* modelled the tip atom by a spherical square well, as opposed to expanding the tip wavefunction in terms of the spherical square well basis set. A more general approach where the spherical square well states are used as a basis set to describe the tip wavefunction is developed in this paper. A number of approaches to describe the tip wavefunction, including an approach which is similar to the one developed in this paper were discussed by Chen (1988).

In this paper the Tersoff–Hamann formalism is extended to include the contributions of tip states with non-zero magnetic quantum numbers to the tunnelling current. It is shown that these states make significant contributions to the tunnelling current and have to be taken into consideration when deriving the analytic form of the tip wavefunction. The basis set will be extended to incorporate the contributions of the tip p states. States of the spherical square well system with an orbital angular momentum number that is greater than one will not be considered in the present work, since the primary purpose of the work is to extend Tersoff and Hamann's s wave model so that the magnitude of the tunnel current can be calculated at nodes of the surface wavefunction. The tunnelling at these points will be dominated by the p_x and p_y states of the tip and adding higher angular momentum components to the tip wavefunction will not substantially affect the results. When the p wavefunctions of the spherical square well can be expressed as derivatives of the s wavefunction. The analytic form of the p states of the spherical square well is given by the following expression

$$\Psi_{pi} = (-C_{pi}/C_s)(1/\kappa)\,\partial\Psi_s/\partial i \qquad i = x, y, z. \tag{8}$$

From (7) and (8) the p states of spherical square well can be expressed as

$$\Psi_{pz} = C_{pz}\int \mathrm{d}\boldsymbol{q}\,\frac{1}{2\pi\kappa}\exp(-(\kappa^2+q^2)^{1/2}|z-z_0|)\exp(\mathrm{i}\boldsymbol{q}\cdot(\boldsymbol{x}-\boldsymbol{x}_0))\kappa R\exp(\kappa R) \tag{9}$$

$$\Psi_{px} = \mathrm{i}C_{px}\kappa R\exp(\kappa R)\int \mathrm{d}\boldsymbol{q}\exp(-(\kappa^2+q^2)^{1/2}|z-z_0|)$$
$$\times\exp(\mathrm{i}\boldsymbol{q}\cdot(\boldsymbol{x}-\boldsymbol{x}_0))q_x/[2\pi\kappa^2(1+q^2/\kappa^2)^{1/2}] \tag{10}$$

where q_x is the x component of the wavevector $\boldsymbol{q}$. The wavefunction Ψ_{py} can be obtained from (10) by replacing x by y.

The ratio of the normalisation constants for the s and p states, $C_s : C_{pi}$, will be taken to be $1:\sqrt{3}$ so that the integrals over the vacuum region of the squared amplitudes of the states are approximately equal.

Each electron that propogates to the end of the STM tip generates a wavefunction in the vacuum which may be expressed in terms of a basis set consisting of the states of the spherical square well. When the wavefunction generated by an electron in the vacuum region is expressed in terms of the s and p states of the spherical square well, the STM tip wavefunction can be written as

$$\Psi_{\nu,\mathrm{tip}} = (\alpha_\nu\Psi_s + \beta_\nu\Psi_{px} + \gamma_\nu\Psi_{py} + \delta_\nu\Psi_{pz}) \tag{11}$$

where ν labels the electron.

The local densities of states of the s, p_x, p_y and p_z tip states at the Fermi energy are determined by the average values of $|\alpha_\nu|^2$, $|\beta_\nu|^2$, $|\gamma_\nu|^2$ and $|\delta_\nu|^2$. If the average values of these quantities are equal then the local densities of states of the s, p_x, p_y, and p_z states of the tip will be approximately equal. For the majority of the discussion in the following section the average values of $|\alpha_\nu|^2|\beta_\nu|^2$, $|\gamma_\nu|^2$ and $|\delta_\nu|^2$ will be taken to be equal to 1. For convenience, these average quantities will be written as $\alpha^2, \beta^2, \gamma^2$ and δ^2 respectively. The effects of varying the relative values of these quantities will be shown in tables in the following sections. The tunnelling matrix elements for the s and p states of the tip are given by

$$M_{s,\mathrm{surf}} = (\alpha h^2/4\pi^2 m)\Psi_{\mathrm{surf}}(\boldsymbol{x}_0, z_0)C_s\exp(\kappa R)\kappa R \tag{12}$$

$$M_{pi,\mathrm{surf}} = -C_{pi}\exp(\kappa R)\kappa R(\lambda/\kappa)(\eta_i h^2/4\pi m)\,\partial\Psi_{\mathrm{surf}}(\boldsymbol{x}, z)/\partial i|_{x=x_0,z=z_0} \tag{13}$$

where $i = x, y$ or z, $\lambda = (\kappa^2 + q^2)^{1/2}$ for the p_z tip state and q_x and q_y respectively for the p_x and p_y tip states, where $\boldsymbol{q}$ represents the surface Bloch vector corresponding to the surface state, and $\eta_i = \beta, \gamma$ or δ.

4. One-dimensional model

The effects of including tunnelling to the p states of the tip from a graphite surface can be illustrated by considering the one-dimensional model used by Tersoff. For the present study, the important feature of the electronic states at the Fermi level of graphite is the presence of nodes in the wavefunction. With a suitable choice of origin, a one-dimensional wavefunction which has the same features as the wavefunctions at the Fermi level in graphite can be written as

$$\Psi_{\text{surf}} = \exp(-\kappa_F z)\sin(k_F x) \tag{14}$$

where k_F is the Fermi wavevector of graphite,

$$\kappa_F = (k_F^2 + \kappa_0^2)^{1/2} \qquad \kappa_0 = 2\pi(2m\Phi)^{1/2}/h,$$

where Φ is the work function of graphite.

Tersoff computed the conductance for this one-dimensional model of the graphite surface by considering only the tunnelling to the s state of the tip. The conductance in this case can be expressed as follows:

$$\sigma = c\sin^2(k_F x_0)\exp(-2\kappa_F z_0) \tag{15}$$

where c is a constant of proportionality that relates the local density of surface states at the centre of the STM tip to the tunnel conductivity. According to (15) when the STM is in the constant tunnel current mode the variation of the vertical distance of the centre of the tip from the surface, z_0, with respect to x_0 can be written as

$$z_0 = [-\ln(\sigma_0/c) + \ln(\sin^2(k_F x_0))]/2\kappa_F \tag{16}$$

where σ_0 is the value of the conductance used in the experiment.

It can be seen that (16) predicts that the corrugation amplitude in the STM image will be infinite since z_0 becomes infinite when $k_F x_0$ is an integer multiple of π. Tersoff argued that the finite size of the Fermi surface would reduce the magnitude of the corrugations to a finite but large value. In a one-dimensional model of the STM tip, only the s, p_x and p_z states of the tip should be retained. When the contributions to the tunnel current from the p_x and p_z states of the tip are included, the sum of the squares of the tunnelling matrix elements for the one-dimensional model of the graphite surface can be expressed as

$$\begin{aligned}|M_{\text{tip,surf}}|^2 = \exp(-2\kappa_F z_0)[&(\alpha^2 h^4)\sin^2(k_F x_0)C_s^2 + (\beta^2 h^4)(k_F/\kappa_0)^2\cos^2(k_F x_0)C_{px}^2 \\ &+ \gamma^2 h^4 \sin^2(k_F x_0)(\kappa_F/\kappa_0)^2 C_{pz}^2 + C_s C_{pz}(\gamma\delta h^4)(\kappa_F/\kappa_0)\cos^2(k_F x_0)] \\ &\times \exp(2\kappa R)(\kappa R)^2/m^2 16\pi^4.\end{aligned} \tag{17}$$

In principle there can be terms in this expression due to interference between the s and p_x channels, and the p_z and p_x channels. However, when contributions to the tunnel current from all the incident electrons in a cylindrically symmetric tip are taken into account these interference terms cancel.

From (17) it can be seen that the relative amplitudes of the tunnelling conductivities for the p_x and the p_z states relative to the s state are of the order

$$\sigma_{px}/\sigma_s = (k_F/\kappa_0)^2 \tag{18}$$

$$\sigma_{pz}/\sigma_s = (\kappa_F/\kappa_0)^2. \tag{19}$$

The p_x state of the STM tip makes a contribution to the tunnel current that is of the same order of magnitude as the contribution from the s state of the tip. The contribution of the p_x (and the p_y for a two-dimensional surface) state of the STM tip to the tunnelling conductivity is usually ignored. This is clearly not justified in the case of the graphite surface. The tunnelling conductivity due to the p_x and p_y states of the tip has the same exponential dependence on the tip–surface distance as the conductivity due to the s and p_z states. Hence the p_x and p_y states make contributions to the total tunnel current which are of the same order of magnitude as those of the s and p_z states and so they have to be taken into consideration in a realistic model of the STM wave function.

The STM image for the one-dimensional model of the graphite surface when tunnelling to the p states is included will now be considered. It will be assumed that the p_x tip state makes the same contribution to the local density of states of the tip as the p_z and the s states and hence that $\alpha^2 = \beta^2 = \delta^2 = 1$. The corrugation function can be written as

$$z_0\{-\ln(\sigma_0/c) + \ln[2\sin^2(k_F x_0) + (\kappa_F/\kappa_0)\sin^2(k_F x_0) + (k_F/\kappa_0)^2]\}2\kappa_F. \tag{20}$$

The values of κ_0, k_F and κ_F for graphite are 1.1 Å^{-1}, 1.7 Å^{-1} and 2.0 Å^{-1} respectively. Substituting these values into (20) gives a corrugation amplitude of 0.23 Å independent of the value of σ_0 or, equivalently, independent of the average tip–surface distance. The STM images for the one-dimensional model of the graphite surface are shown in figure 2. Figure 2(*a*) shows the image when only the s state of the tip is included and figure 2(b) shows the image when the contributions of the s tip state and the p tip states are taken into consideration. The giant corrugations predicted by the s wave only model are completely removed when a more realistic model for the wavefunctions of the STM tip is used.

It is usually assumed that the wavefunctions of an STM tip will be predominantly directed in the forward direction. A basis set consisting of s, p_x and p_z states for the evanescent wavefunctions outside the STM is over-complete. The evanescent wavefunctions are only physically meaningful outside the tip in the vacuum region and as the vacuum region does not extend over a solid angle of 4π the s and p_z basis states are not orthogonal. Hence the choice of $\alpha^2 = \beta^2 = \delta^2 = 1$ in the previous example gives a tip wavefunction that is directed towards the surface which may well be an accurate representation of the wavefunctions of a real STM tip. However it is possible that the s and p_z densities of states of an STM tip may be higher than the p_x and p_y densities of state. The effects of changing the local densities of states of the various angular momentum components of the tip wavefunction in the one-simensional model of the graphite surface can be seen in table 1. As expected, the magnitude of the corrugations in the STM image of the surface increases as the s and p_z densities of states increase with respect to the p_x density of states. However, the magnitude of the corrugations increases relatively slowly with the ratio of the s and p_z densities of states to the p_x density of states.

5. Corrugation amplitude for graphite

The surface layer of graphite has a hexagonal unit cell with a basis of two atoms per lattice point. The usual terminology is to label the atom which is directly over an atom

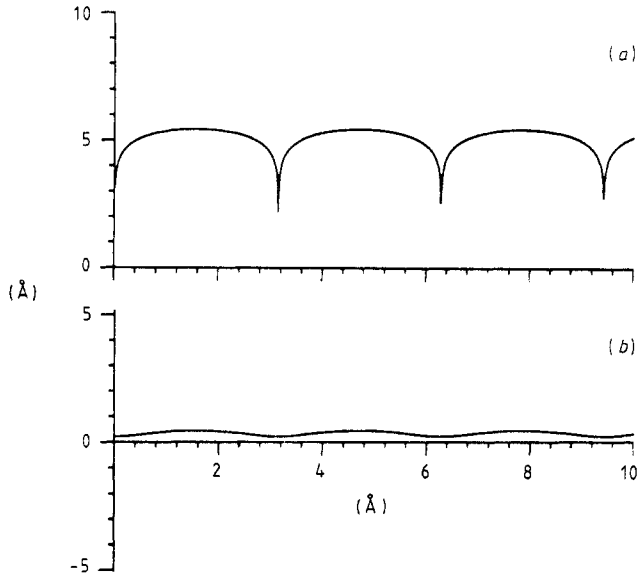

Figure 2. Scanning tunnelling microscope images for the one-dimensional model of the surface of graphite. (*a*) Image obtained when tunnelling only to the s wavefunction of the tip is included. The corrugation amplitude is infinite; the finite corrugation shown in the figure is due to the plotter. (b) Image is obtained when tunnelling to the s, p_x and p_z wavefunctions of the tip is included.

Table 1. The magnitude of the corrugations in the scanning tunnelling microscope image of a one-dimensional model of the graphite surface as a function of the ratio of the s and p_z densities of states of the tip to the p_x density of states.

The ratio of the density of tip p_z and s states to the density of tip p_x states	The corrugation amplitude for the two-plane-wave model
1.00	0.23
2.00	0.40
10.00	0.81
100.00	1.38
500.00	1.77
1000.00	1.94

in the second graphite layer as the α-atom and the other atom as the β-atom. The reciprocal lattice of graphite is hexagonal and the Fermi surface is a point at the corner of the Brillouin zone. The six plane waves represented by the points at the corners of the first Brillouin zone can be divided into two sets of three plane waves such that the three plane waves in each set are separated by reciprocal lattice vectors but there is no interaction between the two sets of plane waves (see figure 3). The wavefunctions at the Fermi level of graphite are, to a good approximation, combinations of these two sets of plane waves. The other plane waves that contribute to the wavefunctions at the Fermi level have much larger wavevectors parallel to the surface which decay much more

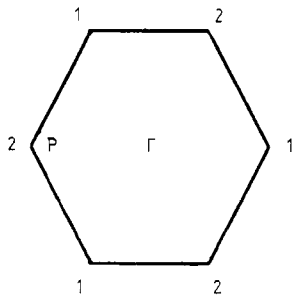

Figure 3. The Brillouin zone of the graphite surface. The Fermi level lies at point P. The numbers indicate the two sets of plane waves that describe the wavefunctions at the Fermi level.

rapidly into the vacuum. Hence these plane waves make a negligible contribution to the wavefunctions at distances that are relevant in the STM and only the three plane waves with the smallest wavevectors parallel to the surface need to be considered. One combination of each of the sets of three plane waves is non-zero on the α-atoms and has nodes on the β-atoms and in the middle of the graphite hexagons. The other combination of the plane waves is non-zero on the β-atoms and has nodes on the α-atoms and in the middle of the graphite hexagons. Tomanek *et al* (1987) have shown that the STM image of graphite at low voltages is sensitive only to the wavefunctions which are non-zero on the β-atoms. This is a result of the energy broadening of the electronic states on the α-atoms induced by the overlap of the wavefunctions onto the second layer atoms. Only when the applied voltage exceeds the energy broadening of the α-atom wavefunctions do the wavefunctions on the α- and β-atoms contribute to the STM image with equal weight. Therefore for applied voltages that are smaller than $\simeq 0.1$ volts only the β-atoms appear in the STM image. At higher voltages both sets of wavefunctions contribute to the STM image and both α- and β-atoms appear in the image.

If it is assumed that an α-atom lies at the origin, the wavefunction that is non-zero on the α-atom is

$$A[\exp(ik_F x) + \exp(ik_F(x - \sqrt{3}y)/2) + \exp(ik_F(x + \sqrt{3}y)/2)] \exp(-\alpha_F z) \tag{21}$$

where A is a normalisation constant and the x axis connects the α-atom at the origin to a neighbouring α-atom. The complex conjugate of (21) gives the α-atom wavefunction which is formed from the other set of three plane waves.

The wavefunction that is non-zero on the β-atoms is

$$\Psi_\beta = A[\exp(ik_F x) + \exp(ik_F(x - \sqrt{3}y)/2) \exp(i2\pi/3) + \exp(ik_F(x + \sqrt{3}y)/2) \exp(-i2\pi/3)] \exp(-\kappa_F z). \tag{22}$$

The complex conjugate of (22) gives the β-atom wavefunction which is formed from the other set of three plane waves.

The matrix elements for tunnelling to the s and p states of the STM tip can be easily calculated from the results presented in the previous section and the tunnel current calculated as a function of the position of the probe. Rather than present a lengthy expression for the magnitude of the tunnel current results will be given for the magnitude of the corrugations expected in an STM image of graphite under a variety of experimental conditions. These results are presented in table 2. The first column in table 2 gives the magnitude of the corrugation expected at low voltages when only the wavefunctions which are non-zero on the β-atoms contribute to the image. In this case the tip will be furthest from the surface when it is positioned above a β-atom and closest to the surface

Table 2. The magnitude of the corrugations in the scanning tunnelling microscope image of graphite as a function of the ratio of the s and p_z densities of states, and of the tip to the p_x and p_y densities of states.

The β-lattice only corrugation amplitude	The α- and β-lattice corrugation amplitude	The ratio of $D(s, p_z)$ to $D(p_x, p_y)$
0.47	0.23	1.00
0.64	0.41	2.00
1.03	0.80	10.00
1.60	1.37	100.00
2.00	1.77	500.00
2.17	1.94	1000.00

when it is either positioned above an α-atom or positioned over the centre of one of the hexagons of atoms. The second column gives the corrugation amplitudes expected at large voltages when the wavefunctions on both α- and β-atoms contribute to the image. In this case the tip will be furthest from the surface when it is positioned above either an α-atom or a β-atom and closest to the surface when it is positioned over the centre of the hexagons. It should be noted that the corrugation amplitude decreases with increasing voltage.

The effect of changing the local densities of states of the s and p_z states of the tip relative to the p_x and p_y states is shown by the values within each column in table 2. As expected, a larger weight in the s and p_z channels relative to the p_x and p_y channels increases the corrugation amplitude. However, it can be seen that an unrealistically large ratio of the local densities of states of the s and p_z tip states relative to the p_x and p_y tip states is required to generate a tunnelling image with a corrugation amplitude of as much as 2 Å. These results show that giant corrugations observed in STM images of graphite cannot be explained by a simple tunnelling model. Hence Tersoff's suggestion that giant corrugations can be present in the STM image of an undistorted graphite surface cannot be correct. It must be concluded that the giant corrugations observed in STM images of the graphite surface can only be due to contact between the tip and the surface or to large elastic deformations induced in the surface by the proximity of the STM tip (Soler *et al* 1986).

6. Summary

It has been shown that tunnelling to the p_x and p_y states of the STM tip can make significant contributions to the tunnelling conductivity. It has been shown that when a realistic model is used for the wavefunctions of the STM tip the corrugation amplitude expected in an STM image of the graphite surface will be small.

Acknowledgments

DL thanks the Science and Engineering Research Council for a studentship and MCP thanks the Royal Society for financial support.

References

Bardeen J 1961 *Phys. Rev. Lett.* **6** 57
Binnig G, Fuchs H, Gerber C H, Rohrer H, Stoll E and Tossati E 1985 *Europhys. Lett.* **31** 1
Binnig G and Quate C F 1986 *Surf. Sci.* **1** 189–190
Chen C J 1988 *J. Vac. Sci. Technol.* A **6** 321
Chung M S, Feuchtwang T E and Cutler P H 1987 *Surf. Sci.* **187** 558
Colton R J, Baker S M, Driscoll R J, Youngquist M G, Baldeschwieler J D and Kaiser W J 1988 *J. Vac. Sci. Technol.* A **6** 349
Elings V and Wudl F 1988 *J. Vac. Sci. Technol.* A **6** 412
Lang N D 1985 *Phys. Rev. Lett.* **55** 230
Mamin H J, Ganz E and Abraham D W 1986 *Phys. Rev.* B **34** 9015
Morita S, Tsukada S and Mikoshiba N 1988 *J. Vac. Sci. Technol.* A **6** 354
Pethica J B 1986 *Phys. Rev. Lett.* **57** 3235
Soler J M, Baro A M, Garcia N and Rohrer H 1986 *Phys. Rev. Lett.* **57** 444
Tersoff J 1986 *Phys. Rev. Lett.* **57** 440
Tersoff J and Hamann D R 1983 *Phys. Rev. Lett.* **50** 1998
—— 1985 *Phys. Rev.* B **31** 805
Tomanek D, Louie S G, Mamin H J, Abraham D W, Thomson R E, Ganz E and Clarke J 1987 *Phys. Rev.* B **35** 7790